Annual CO_2 fluxes from a cultivated fen with perennial grasses during two initial years of rewetting

S. Karki[1,2], T.P. Kandel[1,3], L. Elsgaard[1], R. Labouriau[4] and P.E. Lærke[1]

[1]Department of Agroecology, Aarhus University Interdisciplinary Centre for Climate Change, Tjele, Denmark
[2]Current address: USDA-ARS Delta Water Management Research Unit, Jonesboro, AR 72401, USA
[3]Current address: Noble Research Institute, Ardmore, OK 73401, USA
[4]Department of Mathematics, Aarhus University, Denmark

SUMMARY

Rewetting combined with biomass crop cultivation (paludiculture) has been proposed as a method for reducing carbon dioxide (CO_2) emissions from drained peatlands. This field experiment compared CO_2 fluxes from drained (control) and rewetted experimental plots in a temperate fen under reed canary grass cultivation over two successive years. The annual weighted mean water table depth from soil surface (WTD) during the study period was 9, 3 and 1 cm in control, semi-flooded and flooded plots, respectively. There were no significant effects of WTD treatment on biomass yields. The choice of response model for CO_2 fluxes influenced annual estimates of ecosystem respiration (ER) and gross primary production (GPP), but all models showed that ER and GPP decreased in response to rewetting. The resulting net ecosystem exchange (NEE) of CO_2, derived by combining eight ER and eight GPP models, varied widely. For example, NEE (expressed as CO_2-C) ranged from -935 to -208 g m^{-2} yr^{-1} for the flooded plots. One set of ER and GPP models was selected on the basis of statistical criteria and showed insignificant differences in NEE between the three water table treatments (-537 to -341 g CO_2-C m^{-2} yr^{-1}). Treatment effects on CO_2 emission factors, calculated as the sum of NEE and C export in harvested biomass (58–242 g CO_2-C m^{-2} yr^{-1}), were similarly insignificant. Thus, the results indicated that varying WTD within this narrow range could influence both ER and GPP without altering the net emissions of CO_2.

KEY WORDS: ecosystem respiration, gross primary production, paludiculture, reed canary grass

INTRODUCTION

Peatlands are important in the global carbon cycle because they store approximately 600 Pg of carbon (C) (Gorham 1991, Yu *et al.* 2011). However, drainage and subsequent use for agriculture and forestry have drastically altered the C storage functions of many peatlands during the last century (Wichtmann *et al.* 2016). In drained peat soils that are used for agriculture, peat oxidation and mineralisation processes contribute to large emissions of carbon dioxide (CO_2) resulting in peat subsidence rates of a few to 50 mm per year, depending on drainage intensity and climatic conditions, with the highest subsidence rates occurring in the tropics (Leifeld *et al.* 2011, Hooijer *et al.* 2012). Globally, the annual emissions of CO_2 from drained peatlands are estimated at 0.78 Pg, which is equivalent to 25 % of the net CO_2 emissions from the agriculture, forestry and land use sector (Tubiello *et al.* 2016). However, many peatlands which have been drained for agriculture (at least in northern Europe) are currently being abandoned due to peat degradation, declining productivity and the high cost of drain maintenance (Biancalani & Avagyan 2014, Kløve *et al.* 2017). To further reduce peat degradation and CO_2 emissions, novel yet socioeconomically viable approaches to the management of agricultural peatlands are needed (Joosten *et al.* 2015).

Paludiculture is an innovative land use concept for poorly drained and rewetted peatlands which involves harvesting natural or cultivated biomass for energy or industrial uses (Joosten *et al.* 2015, Wichtmann *et al.* 2016). While such management allows productive use of the land to continue, the shallower water table may restrict exposure of the peat to oxygen (O_2) - which diffuses more slowly in water-filled pores than in air-filled pores (Moldrup *et al.* 2000, Dinsmore *et al.* 2009, Karki *et al.* 2015b) - and thus result in reduced peat degradation and CO_2 emissions. Paludiculture may also improve ecosystem services such as nutrient and water retention and biodiversity (Wichtmann *et al.* 2016). Although it has been recommended as a promising management option for drained peatlands in recent reports of the Food and Agriculture Organization of the United Nations (Biancalani & Avagyan 2014) and the Inter-governmental Panel on Climate Change (IPCC

 DOI: 10.19189/MaP.2017.DW.322

2014), there is still limited quantitative information on the effectiveness and optimisation of paludiculture as a tool for mitigating CO_2 emissions (IPCC 2014, Günther *et al.* 2015, Karki *et al.* 2016). So far, most studies of CO_2 fluxes from paludicultures have focused on rewetted peatlands with natural vegetation and low-input management such as no fertiliser and a single annual harvest (Beetz *et al*. 2013, Günther *et al.* 2015). For paludiculture to become socioeconomically viable, it is likely that more intensive management and dedicated biomass crops will be needed in the future (Günther *et al.* 2015). Karki *et al*. (2016) recently simulated intensive paludiculture with multiple harvests (cuts) and fertiliser applications each year, in a mesocosm study with newly established reed canary grass (RCG; *Phalaris arundinacea* L.). This study reported higher net uptake of CO_2 for completely rewetted peat soils than for drained and partially rewetted soils with constant water table depth below ground level (WTD). To substantiate these results, more comprehensive studies are needed to quantify the CO_2 emissions from rewetted sites where, for example, lateral water flow, fluctuating water table and *in situ* biomass development occur.

In the present study we measured CO_2 fluxes on a fen peatland that had been rewetted to various degrees and cultivated with RCG in a fertilised two-cut management system during two consecutive years after rewetting. The objectives of the study were to:

(i) quantify and compare the effects of different water table levels (treatments) on annual CO_2 balances and biomass yields under perennial grass cultivation; and

(ii) address the consistency of net annual CO_2 balances resulting from different modelling approaches.

METHODS

Study site and cropping history

The study site was a drained and cultivated fen peatland located in the Nørreå river valley in central Jutland, Denmark (56° 27′ 32″ N, 9° 40′ 40″ E; 3 m a.s.l.), with temperate Atlantic climate. Average long-term (1985–2015) annual air temperature was 7.9 °C, total annual precipitation 650 mm and total annual global radiation 3540 MJ m^{-2}, equivalent to 1868 mmol m^{-2} of photosynthetically active radiation (PAR). Global radiation was converted to PAR using a conversion factor of 1.9 µmol J^{-1} (Al-Shooshan 1997). The fen was a minerotrophic wetland that received nutrients from the surrounding moraine landscape through drainage and surface runoff (Knadel *et al.* 2011, Walpersdorf *et al.* 2013).

The fen was drained for agricultural use by establishing open ditches in the early 20th century. Tile drain pipes at 60–80 cm depth were added in 1967. Continued agricultural use resulted in peat subsidence, and the drainage was reinforced with PVC drain pipes at 60–80 cm depth in 1985. In recent decades, the site was used for spring barley (*Hordeum vulgare* L.) cropping, either continuously or in rotation with grass-clover. In 2011, the soil was ploughed and sown with RCG (cultivar Bamse) for experimental purposes.

Details of soil properties at the study site were presented by Kandel *et al.* (2013b). Briefly, peat depth was >1 m and the topsoil (0–20 cm) was characterised by bulk density 0.29 g cm^{-3}, organic C content 36.3 %, total nitrogen (N) content 3.0 % and pH(H_2O) in the range 6.1–7.1. Bulk density decreased with depth because the peat in deeper layers was less decomposed than the topsoil.

Study design and crop management

The study was conducted from March 2015 to February 2017. Hereafter, the period between March 2015 and February 2016 is referred to as Year 1 and the period between March 2016 and February 2017 is referred to as Year 2. The study was planned as a split block design with four blocks (14 × 18 m) and two plots with different water table treatments, representing control and continuous rewetting (water table close to the soil surface), in each block (Figure 1). A confinement was made around the 'rewetted' plot in each block using inert plastic strip (0.3 cm thick, 30 cm wide; Danbox Denmark ApS, Langå, Denmark). The plastic strip was inserted vertically to 25 cm depth leaving 5 cm above ground level to control surface runoff. Rewetting was accomplished by pumping water from a drainage ditch into elevated tanks, whence it could flow continuously (by gravity) through 4 cm diameter PVC tubing to the plots (Figure 1). The resulting WTD in each block and plot was influenced by the topography of the study area and the distance of the block from the drainage ditch. The four confined plots were always intentionally flooded, and the two unconfined (control) plots close to the drainage ditch (Figure 1) also had a high degree of rewetting after mid-June in Year 1 due to subsurface intrusion of water from the flooded plots. Therefore, the resulting water table treatments were designated as 'flooded' for the confined plots ($n = 4$), 'semi-flooded' ($n = 2$) for two of the unconfined plots, and 'control' ($n = 2$) for the other two unconfined plots (farthest from the drainage ditch). Thus, the study followed an unbalanced split block design with three water table

 DOI: 10.19189/MaP.2017.DW.322

treatments. Two 'GHG collars' (details given later) were installed in each plot.

Fertilisation and harvest events in the years before and during the study period are presented in Figure 2. Crop management during the study period (2015–2017) was optimised to enhance the quality and quantity of biomass for biogas production, which required multiple harvests of green (above-ground) biomass and repeated fertiliser applications (Kandel *et al*. 2013a, 2013c). Standard mineral fertiliser (N-P-K at 80-13-62 kg ha^{-1}) was applied to all plots on 23 March 2015, five days prior to the start of flooding. The biomass inside the GHG collars was harvested manually on 15 June and fertilised again on 24 June. The regrowth was then harvested on 01 October to represent a two-cut management regime. In 2016, all plots were fertilised on 31 March during spring growth and biomass was harvested on

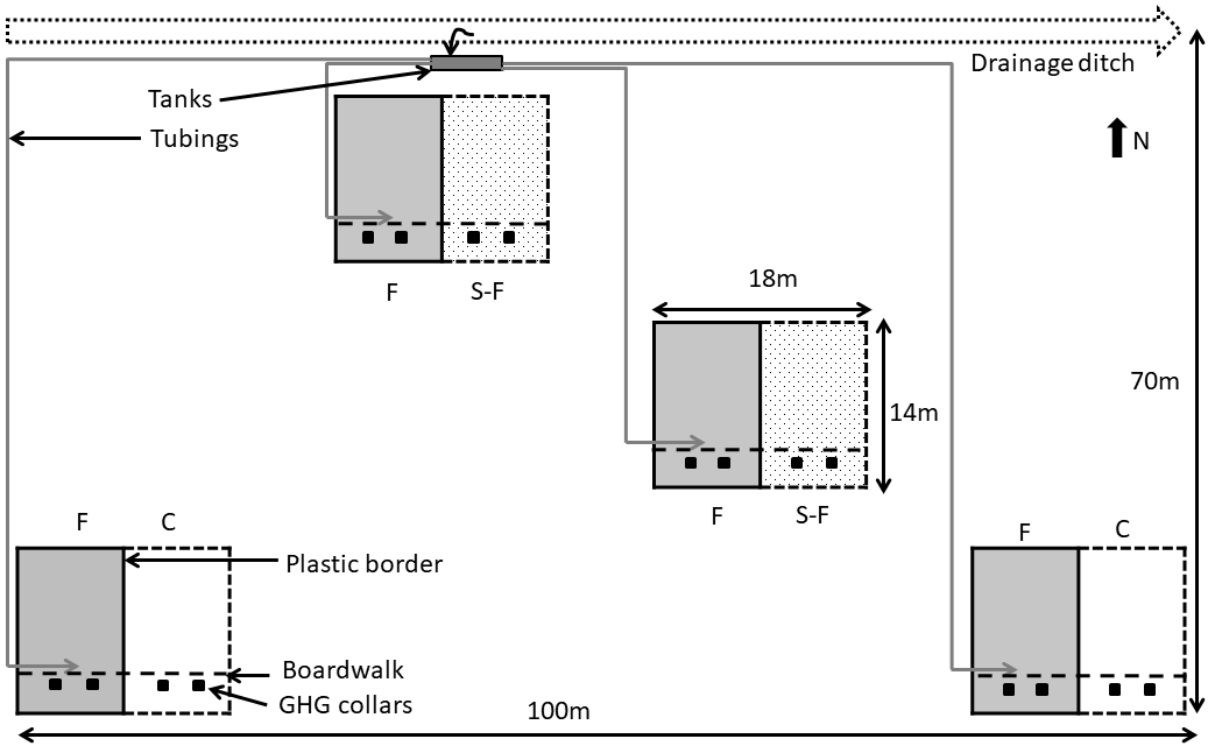

Figure 1. Layout of the field experiment. Four blocks (14 × 18 m) were divided into two plots (14 × 9 m) to impose flooding treatments. The water table treatments were flooded (F), semi-flooded (S-F), and control (C). Water was pumped from the drainage ditch (large dotted arrow) to the tank. The grey arrows indicate pipelines connecting water tanks to the flooded plots confined by plastic borders. Black squares at the southern end of each plot indicate the collars (0.55 × 0.55 m) installed for gas flux measurements.

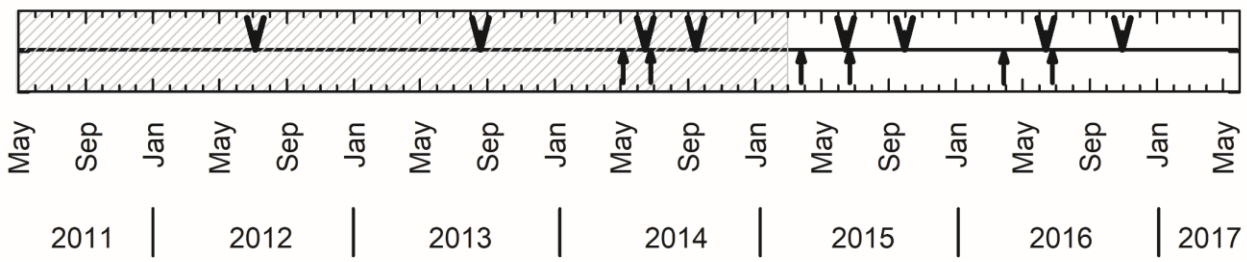

Figure 2. Timeline of harvest (arrowheads) and fertilisation (upward arrows) before (May 2011 – February 2015; hatched area) and during the study period (March 2015 – March 2017). The study site was ploughed and sown with reed canary grass in May 2011. The experimental rewetting of the flooded plots started on 28 March 2015. Plots were fertilised with standard mineral fertilisers (80-13-62 kg N-P-K ha^{-1}).

 DOI: 10.19189/MaP.2017.DW.322

13 June. After subsequent fertilisation on 21 June, a final harvest was taken on 31 October. Dry matter (DM) content of the biomass from each harvest was determined by oven drying all biomass inside the collars to constant weight at 60 °C. Biomass yields from a collar at the two harvest dates in each year were summed to obtain total annual yield.

CO_2 flux measurements

Three weeks prior to the first CO_2 flux measurements, two white PVC collars (55 × 55 × 11 cm) were inserted into the soil to a depth of 10 cm with a distance of 1 m between them. At collar installation (09 February 2015), the growing season had not yet started but the plots were covered with short green grass. Each collar had a 4 cm wide outer flange that was kept parallel to the soil surface and served to support the chamber top during flux measurements (Elsgaard *et al.* 2012). The collars remained in place for the entire study period. A PVC boardwalk was placed alongside the collars to reduce disturbance of soil gas profiles during measurements.

Fluxes of CO_2 were measured using a transparent chamber top (60 × 60 × 41 cm) made from Plexiglas and equipped with a temperature control unit, cooling and mixing fans, and a PAR sensor (190-SA; Li-Cor Inc., Lincoln, NE, USA). Details of the chamber design and data acquisition are described by Elsgaard *et al*. (2012). Briefly, the chamber was connected by 4 mm inlet and outlet tubing to a portable analysing unit where CO_2 and H_2O concentrations were measured at one-second intervals using an infrared gas analyser (Li-840A; Li-Cor Inc.). A chamber extension with the same dimensions as the chamber top was used later in the growing season, when plant height exceeded the height of the chamber. Fluxes were generally measured at two-week intervals from 05 March 2015 to 03 March 2017, but more frequently during periods of rapid growth.

During each measurement campaign, CO_2 fluxes at the 16 collars were measured at four levels of PAR, imposed by shrouding as described by Kandel *et al.* (2017). First, the CO_2 flux was measured for one minute under fully transparent conditions; this flux represented net ecosystem exchange (NEE) at the prevailing PAR. Then the chamber was covered with black netting to block ~ 50 % PAR and the vegetation was allowed to adapt to the new PAR level for one minute before a one-minute flux measurement. During the adaptation period, the side of the chamber facing the wind was lifted 15–20 cm from the collar to bring the CO_2 concentration back to atmospheric level. On rare occasions when there was no wind, a stream of air was created by waving a sheet of cardboard outside the chamber opening. A second layer of black netting was then added to block a total of ~75 % PAR, and the procedure was repeated. Finally, the chamber was covered with a white opaque cover to block 100 % PAR and the CO_2 flux (i.e., ecosystem respiration, ER) was measured after one minute of dark adaptation.

Fluxes were measured between 10:00 and 13:00 hrs. Measurement dates were normally fixed in advance and campaigns were carried out under the prevailing cloud conditions (sunny, partially cloudy or overcast days) but not on rainy days. On partially cloudy days, conditions of (nearly) constant PAR were achieved for individual measurements by timing chamber deployments with consideration of the movement of clouds across the sun.

Fluxes were calculated using the MATLAB® (MathWorks, Inc., Natick, MA, USA) protocol by Kutzbach *et al.* (2007), applying a water vapour correction. Data from the first ten seconds after chamber deployment were discarded as a dead-band. Linear (rather than non-linear) regression was used for flux calculation as it generally gives more stable results for short enclosure periods (Kandel *et al.* 2016).

Ratio vegetation index

Aboveground biomass development in each collar was monitored during the study period by measuring canopy light reflectance using a SpectroSense 2+ fitted with SKR1850 sensors (Skye Instruments, Powys, UK) as described by Kandel *et al.* (2017). The sensors were held at nadir angle at a height of 1 m above the ground, to cover a 0.15 m^2 area inside the collars. The sensors measured incident and reflected red (R) light at 640 ± 10 nm and near-infrared (NIR) light at 778 ± 16 nm (Görres *et al.* 2014). The ratio vegetation index (RVI) was then calculated as $(NIR_r/NIR_i)/(R_r/R_i)$, where the subscripts *i* and *r* denote the incident and reflected radiation, respectively. On all measurement days, reflectance was measured just before chamber deployment to record the reflectance from undisturbed biomass. Vegetation indices measured as canopy reflectance (such as RVI in the current study) combine information about the amount of vegetation and its photosynthetic activity and have been considered as proxies for photosynthetically active biomass (Wiegand & Richardson, 1984).

Environmental variables

Air temperature and PAR during chamber deployment were recorded by sensors inside the chamber (Elsgaard *et al.* 2012). Continuous hourly measurements of air temperature and PAR were obtained from the climate station of Aarhus University (Foulum, Denmark) 7 km from the study

 DOI: 10.19189/MaP.2017.DW.322

site. Soil temperature at 5 cm depth was recorded at hourly intervals using HOBO temperature data loggers (Model UA-001-64; Onset Computer Corporation, Bourne, MA, USA) installed in one plot for each treatment.

Volumetric water content (VWC) at 0–20 cm soil depth inside each collar was measured manually on flux measurement days when the soil was not frozen using permanently installed time domain reflectometer (TDR) probes (Plauborg *et al.* 2005). Relative VWC (i.e., proportion of maximum value measured under flooded conditions) for each collar was used to represent the water-filled pore space (Shrestha *et al*. 2014). Natural fluctuation of water table depth in the study area was monitored at hourly intervals from May 2015 in a PVC tube (5 cm diameter, 150 cm long; perforated all the way down from 5 cm below soil surface) installed about 50 m from the nearest plot, using a PTX 1730 pressure transducer sensor (GE Druck, Leicester, UK). Water table depth was also measured manually during each flux measurement campaign, in similar tubes installed within one metre of each collar.

Flux modelling and annual CO_2 fluxes

The CO_2 fluxes were partitioned into light-dependent GPP and light-independent ER. GPP was estimated as (NEE - ER), where ER is always positive (≥ 0) and GPP is always negative (≤ 0); hence the sign of NEE is positive when there is a net flux of CO_2 to the atmosphere (Kandel *et al.* 2017). GPP was calculated for each of the three NEE fluxes in a measurement cycle (at different PAR levels) by subtracting the corresponding ER measurement. Cumulative annual fluxes were derived from separate modelling of GPP and ER. Annual NEE was then calculated as (GPP + ER). CO_2 emission factors were then calculated by summing NEE and the C exported in harvested biomass (Renou-Wilson *et al.* 2014, Renou-Wilson *et al.* 2016, Tiemeyer *et al.* 2016).

GPP and ER were modelled with eight deductive response models each. Several deductive response models were compared using the same flux data, as model selection can markedly influence annual estimates of ER and GPP (Görres *et al.* 2014, Huth *et al.* 2017, Kandel *et al.* 2017). The models were selected from previous studies and included PAR (for GPP models only), temperature and RVI as driving variables (Tables 1 and 2). All models (except GPP Model 1) were fitted for each treatment by pooling the entire dataset. For GPP Model 1, fitting was done for each treatment and measurement date (Elsgaard *et al*. 2012). A few winter measurement dates were merged to achieve convergence of the Model 1

Table 1. Ecosystem respiration (ER) models adapted or modified from previous studies and used with the present dataset.

Model	Model structure for ER	References and comments
1	$R_{10} \times e^{\left(E_0\left(\frac{1}{T_{10}-T_0}-\frac{1}{T-T_0}\right)\right)}$	Lloyd & Taylor 1994, Elsgaard *et al.* 2012, Beetz *et al.* 2013, Günther *et al.* 2015, Minke *et al.* 2016, Poyda *et al.* 2016.
2	$R_0 \times e^{bT}$	Soini *et al.* 2010, Vanselow-Algan *et al.* 2015, Järveoja *et al.* 2016.
3	$(R_0 + (\alpha \times RVI)) \times e^{bT}$	Kandel *et al.* 2013b.
4	$(R_{10} + (\alpha \times RVI)) \times e^{\left(E_0\left(\frac{1}{T_{10}-T_0}-\frac{1}{T-T_0}\right)\right)}$	Modified version of Model 1 with RVI to model the influence of biomass on ER as in Model 3.
5	$R_{10} \times e^{\left(E_0\left(\frac{1}{T_{10}-T_0}-\frac{1}{T-T_0}\right)\right)} + (\alpha \times RVI)$	Mäkiranta *et al.* 2010, Karki *et al.* 2016.
6	$(R_0 + (\alpha \times RVI)) \times \left(\frac{47.9}{1+e^{\left(\frac{106}{T+18.3}\right)}}\right)$	Kandel *et al.* 2017, 2018, 2019.
7	$R_0 + (b \times T) + (\alpha \times RVI)$	Wilson *et al.* 2007. RVI was used instead of vascular green area.
8	$e^{bT} + (\alpha \times RVI)$	Urbanová *et al.* 2013. RVI was used instead of vascular green area.

R_{10} is respiration at 10 °C, E_0 is the ecosystem sensitivity coefficient, T_{10} is a reference temperature at 10 °C, T is the air temperature (°C), T_0 is a theoretical zero respiration temperature, here fixed to -46 °C (Lloyd &Taylor 1994), R_0 is respiration at 0 °C, b is a temperature sensitivity parameter, RVI is the ratio vegetation index, α is a scaling parameter of RVI. All model parameters obtained with the different models were significant ($P < 0.05$).

algorithm. GPP and ER models were fitted using non-linear regression in SigmaPlot 11 (Systat Software Inc., San Jose, CA, USA).

Extrapolation of ER to annual fluxes was based on the estimated model parameters in combination with a continuous time series of air temperature and linearly interpolated (to hourly time steps) RVI. Extrapolation of GPP followed a similar approach based on hourly PAR and linearly interpolated RVI. For all models that included RVI (i.e., all models except GPP Model 1), extrapolation was carried out using one set of model parameters for each treatment. For GPP Model 1, a linear development of model parameters between measurement campaigns was assumed. The α and GPP_{max} values in GPP Model 1 (Table 1) were set to -0.0001 and -0.01 µg m^{-2} s^{-1}, respectively, after biomass harvests (Beetz *et al.* 2013).

The fit of individual models was evaluated on the basis of Nash-Sutcliffe modelling efficiencies (NSE), where NSE values closer to unity indicate higher accuracy (Nash & Sutcliffe 1970). Furthermore, accordance between modelled and measured fluxes was evaluated using different statistical indicators such as paired *t*-tests, correlation coefficient (*r*) and simultaneous *F*-test for unit slope and zero intercept (Haefner 2005, Piñero *et al*. 2008). The statistical performance of the model was rated from good to excellent, based on Hoffmann *et al*. (2015). Informed by these evaluations, we selected one ER and one GPP model as a basis for further comparisons of water table treatments with annual CO_2 fluxes. The selected models were used to estimate GPP and ER individually for each collar to provide insights about spatial variations in the annual CO_2 emissions.

Statistical analyses

The effects of WTD treatments, year and time of harvest (first and second cut) on the biomass yield were analysed using the following linear mixed model:

$$M_{ycbtr} = \mu_{yct} + B_b + U_{\mathrm{btr}} + E_{\mathrm{ycbtr}} \quad [1]$$

where M_{ycbtr} is the biomass yield of the r^{th} (r = 1, 2) repetition (collar) at the b^{th} block (b = 1, 2, 3, 4) of the c^{th} time of cut (c = 1, 2) in the y^{th} year (y = 1, 2) of an experimental unit subject to the t^{th} WTD treatment (t = control, semi-flooded and flooded). The term

Table 2. Gross primary production (GPP) models adapted or modified from previous studies and used with the present dataset.

Model	Model structure for GPP	References and comments
1	$\frac{GPP_{\max} \times \alpha \times PAR}{GPP_{\max} + \alpha \times PAR}$	Thornley & Johnson 1990, Elsgaard *et al.* 2012, Beetz *et al.* 2013, Günther *et al.* 2015, Vanselow-Algan *et al.* 2015, Minke *et al.* 2016, Poyda *et al.* 2016.
2	$\frac{GPP_{\max} \times RVI \times \alpha \times PAR}{(GPP_{\max} \times RVI) + (\alpha \times PAR)}$	Kandel *et al.* 2013a, Görres *et al.* 2014, Karki *et al.* 2016.
3	$\frac{GPP_{\max} \times RVI \times \alpha \times PAR}{(GPP_{\max} \times RVI) + (\alpha \times PAR)} \times \mathrm{FT}$	Kandel *et al.* 2017.
4	$\frac{GPP_{\max} \times PAR}{\kappa + PAR} \times RVI$	Wilson *et al.* 2007, 2013, Soini *et al.* 2010, Urbanová *et al.* 2013. RVI was used instead of vascular green area or green area index.
5	$\frac{GPP_{\max} \times PAR}{\kappa + PAR} \times \left(\frac{RVI}{RVI + a} \right)$	Wilson *et al.* 2013, Renou-Wilson *et al.* 2014, 2016. RVI was used instead of leaf area index, vascular green area, or green area index.
6	$\frac{GPP_{\max} \times PAR}{\kappa + PAR} \times (1 - \mathrm{e}^{(-a \times RVI)})$	Urbanová *et al.* 2013. RVI was used instead of vascular green area.
7	$\frac{GPP_{\max} \times PAR}{\kappa + PAR} \times \left(\frac{RVI}{RVI + a} \right) \times \mathrm{FT}$	Modified version of Model 5 where a temperature dependence function (FT) was included as in Model 3.
8	$\frac{GPP_{\max} \times PAR}{\kappa + PAR} \times (a + RVI)$	Soini *et al.* 2010. RVI was used instead of vascular green area.

GPP_{max} is the asymptotic maximum rate of GPP at increasing photosynthetically active radiation (PAR), α is the initial light response efficiency in the original Model 1, RVI is the ratio vegetation index, FT is a temperature dependent function of photosynthesis set to 0 below - 2 °C and 1 above 10 °C and with an exponential increase between - 2 and 10 °C, κ is the PAR value at which GPP reaches half of its maximum (half saturation constant), and a is model-specific parameter.

 DOI: 10.19189/MaP.2017.DW.322

μ_{yct} is a fixed effect representing the mean biomass yield of the c^{th} time of cut at t^{th} WTD treatment in the y^{th} year. B_b, U_{btr} and E_{ycbtr} are independent random components representing block, experimental unit as the r^{th} repetition of the p^{th} plot ($p = 1, 2$) and the residual variation, respectively. The experimental design adopted (see Figure 1) is such that the plots are identified in the model by the t^{th} management of the b^{th} block. A similar model without time of harvest was used to analyse the effects of WTD treatments and year on annual cumulative CO_2 fluxes, i.e., ER, GPP, NEE and the CO_2 emission factor. The statistical inference of the linear mixed models was performed using the 'lme4' package in R (R Core Team 2016). The basic assumptions of normality and variance homogeneity were verified using the Shapiro-Wilks test and the Bartlett test, respectively, applied to the raw residuals; no significant departures from these assumptions were found. Post-hoc analyses grouping the treatments for each year and comparing the two years for each treatment were performed using the package 'pairwiseComparisons' in R (Labouriau 2018); all post-hoc tests were corrected for multiple testing using the false discovery rate method (Benjamini & Hochberg 1995, Benjamini & Yekutieli 2001).

RESULTS

Climate conditions

In both study years, mean annual temperature (8.3 °C in Year 1, 8.7 °C in Year 2) and total annual precipitation (821 mm in Year 1, 755 mm in Year 2) exceeded the long-term (1985–2015) average values for the area (7.9 °C, 650 mm). The study years differed mainly in terms of mean temperature during the growing season (March–September), which was 10.9 °C in Year 1 and 12.1 °C in Year 2 (Figure 3a). Although total precipitation during the growing season was similar in the two years (Figure 4a), Year 2 had more precipitation in April and July and markedly less in September (Figure 3b). Global radiation was close to the long-term average in both Year 1 (3580 MJ m^{-2}, equivalent to 1889 mmol m^{-2} PAR) and Year 2 (3440 MJ m^{-2}, equivalent to 1816 mmol m^{-2} PAR) (Figure 3c).

The average soil temperatures at 5 cm soil depth for the flooded, semi-flooded and control plots were 8.6, 9.0, and 8.8 °C, respectively, in Year 1; and 9.0, 9.3, and 9.1 °C, respectively, in Year 2 (data not shown). The highest soil temperatures were observed in the semi-flooded plots and the lowest in the flooded plots, but they differed by less than 0.4 °C in both years.

Water table and soil moisture content

The mean position of the water table in the study area (~ 50 m from the nearest plot) was about 15 cm below the soil surface in both years. During growing periods, the water table generally fluctuated between 5 cm and 40 cm (mean 18 cm) below the soil surface in Year 1, and between 8 cm above and 55 cm below the soil surface (mean 20 cm below) in Year 2 (Figure 4b).

The mean annual WTD in the experimental plots (treatments) differed slightly and corresponded to two-year weighted averages of 1, 3 and 9 cm below the soil surface for the flooded, semi-flooded and control plots, respectively (Figure 4c). The water table was always at the soil surface in the flooded plots, except for few days in March and September in

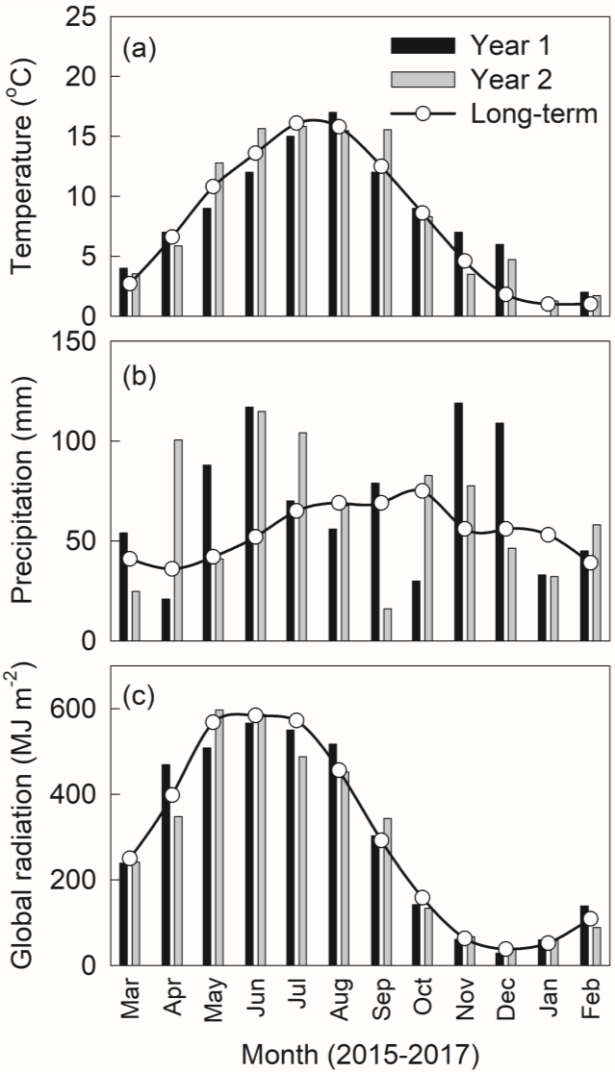

Figure 3. Mean monthly (a) air temperature, (b) precipitation and (c) global radiation in the study area during Year 1 (March 2015 – February 2016), Year 2 (March 2016 – February 2017), and during the long-term period 1985–2015.

 DOI: 10.19189/MaP.2017.DW.322

Year 2 when it dropped to 10 cm below the soil surface due to failure of the pumping system. The WTD treatment difference between the plots was more evident during the growing periods than during the non-growing periods (October–February). Thus, the mean WTD among the treatments in the growing periods was 1, 5 and 14 cm for the flooded, semi-flooded and control plots, respectively (Figure 4c). During winter, the rewetting system failed periodically due to frozen water in the tanks and tubing. However, the water table was mostly at the soil surface in the whole study area during these periods.

Relative VWC in control plots ranged from around 0.76 to 0.96 with a mean of 0.87 for both years (Figure 4d). Overall, the treatment effects were moderate but, as also seen for WTD dynamics, VWC differences among the treatments were observed during the growing periods; VWC was always higher in the flooded plots than in the control plots.

Biomass development and yield

Dynamics of RVI were similar for all treatments until the first harvest in both years (Figure 5c). After the first harvest, RVI in the flooded plots was lower than

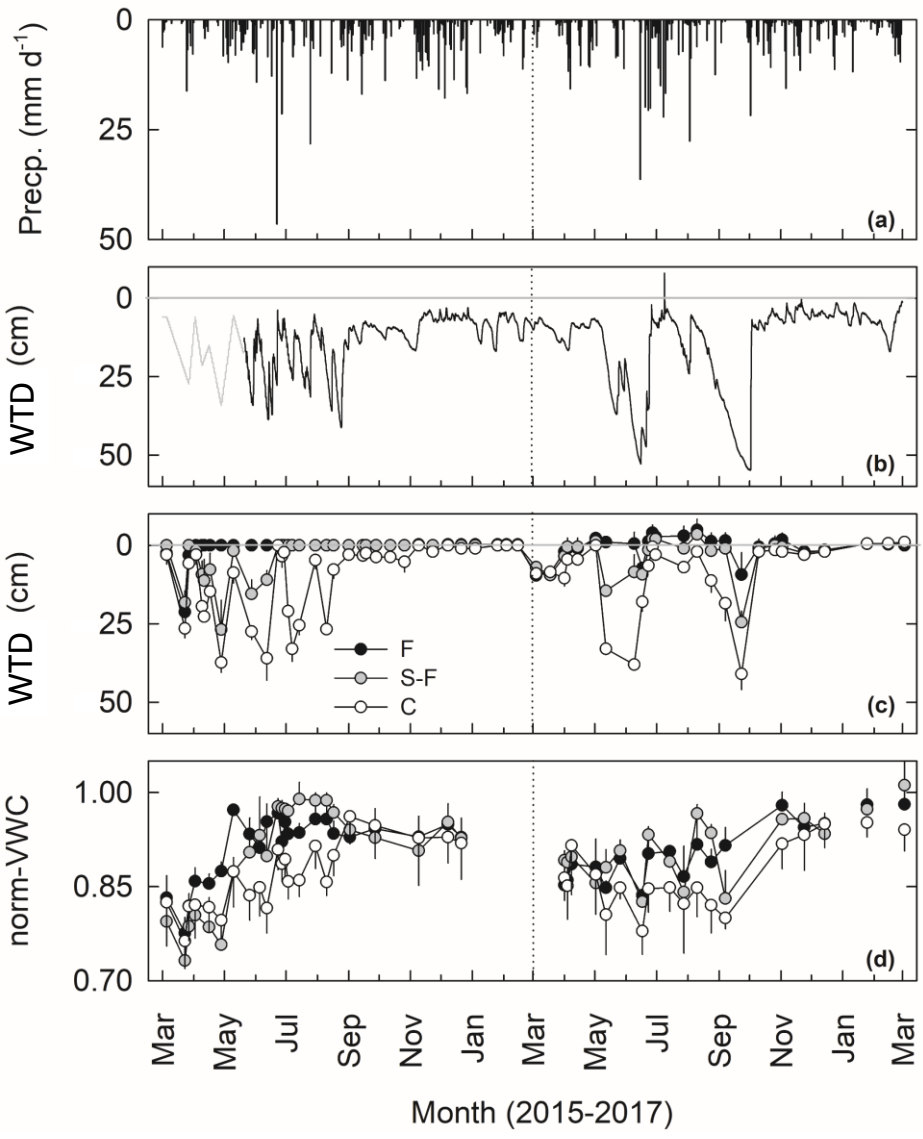

Figure 4. (a) Daily precipitation, (b) natural dynamics of water table depth below soil surface (WTD) in the study area, (c) dynamics of WTD in flooded (F), semi-flooded (S-F) and control (C) plots, and (d) volumetric water content (VWC) measured at 0–20 cm soil depth and normalised relative to the (collar-wise) maximum volumetric water content (norm-VWC). WTD (b) was at first measured manually at 1–2 week intervals (grey line) and then automatically at intervals of one hour (black line). Error bars in (c) and (d) represent the spatial variation (standard error, n = 4 for F plots and n = 2 for S-F and C plots). Unidirectional error bars are shown for clarity. The vertical dotted line separates the two study years.

 DOI: 10.19189/MaP.2017.DW.322

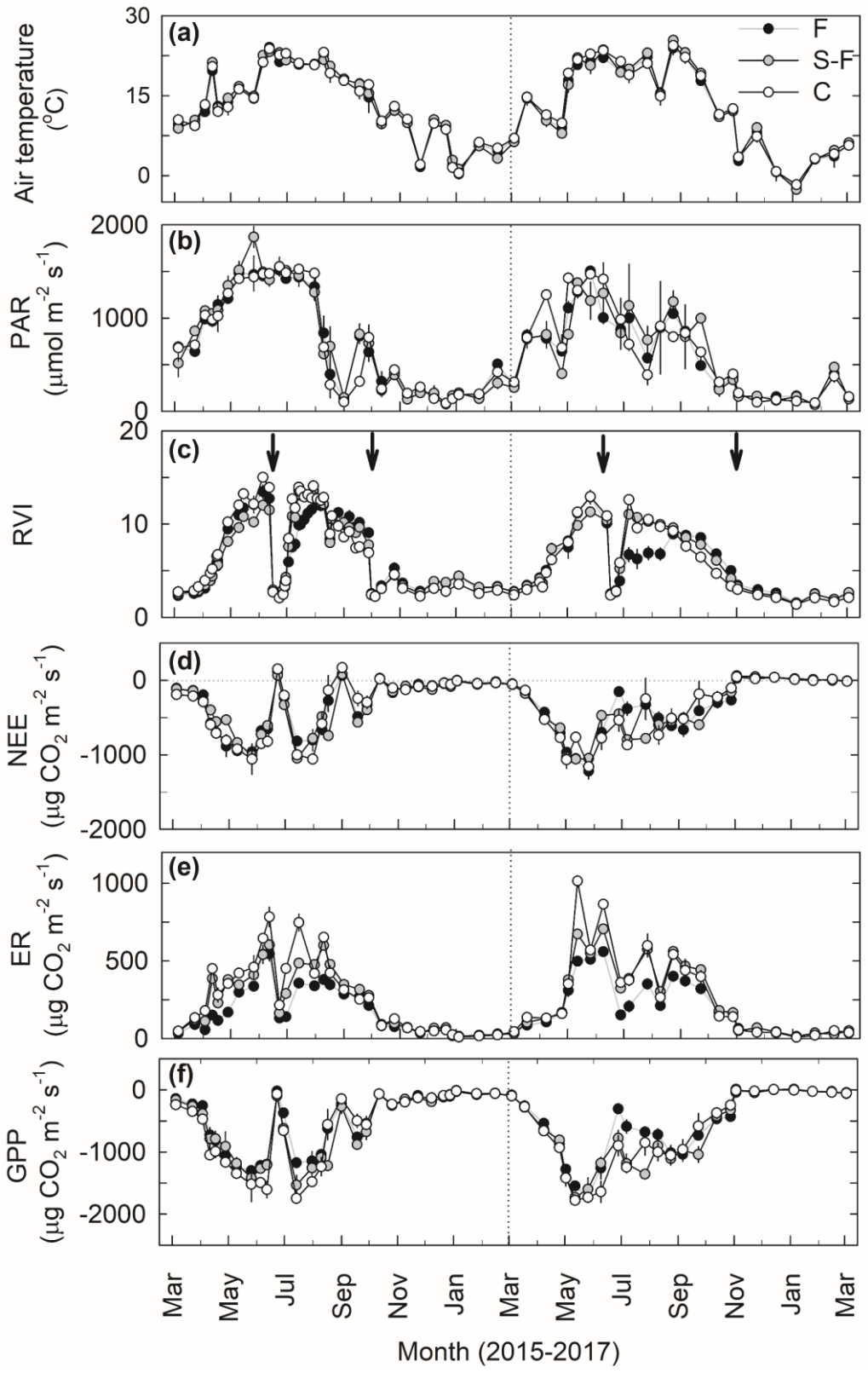

Figure 5. (a) Mean air temperature during flux measurements, (b) photosynthetically active radiation (PAR) inside fully transparent chamber at prevailing light conditions during flux measurements, (c) ratio vegetation index (RVI) as a proxy of green biomass, (d) mid-day net ecosystem exchange (NEE) at prevailing PAR, (e) mid-day ecosystem respiration (ER), and (f) gross primary production (GPP) calculated as GPP = NEE - ER. Data are shown for flooded (F), semi-flooded (S-F) and control (C) plots. Error bars represent the spatial variation (standard error, n = 4 for F plots and n = 2 for S-F and C plots). Arrows indicate harvest events. The dotted vertical line demarks the two study years.

 DOI: 10.19189/MaP.2017.DW.322

in the semi-flooded and control plots at the beginning of the regrowth period, as grasses were more impaired (and partly killed) in the flooded plots. When new biomass eventually emerged in the flooded plots, this regrowth subsequently reached similar RVI peaks as seen for semi-flooded and control plots. Yet, as regrowth of grasses in the flooded plots started later, they also reached senescence later. After the final harvest in autumn, regrowth of grasses other than RCG was observed (albeit weak) and the plots stayed green during winter. When comparing biomass growth between the two study years, the most notable difference was observed after the first harvest where RVI was lower in Year 2, especially in the flooded plots.

There was no significant effect of WTD treatments on biomass yield (P = 0.175), but the yields in the two years were significantly different (P < 0.001), i.e., on average 19 % lower in Year 2 than in Year 1 (Figure 6). This was mainly caused by yield reduction of the biomass in the second cut in Year 2. There was no significant effect (P = 0.163) of different cuts (i.e., first and second cut) on biomass yield in Year 1, but the biomass yield in the second cut in Year 2 was significantly lower than in the first cut (P < 0.001) and also significantly lower than in the second cut in Year 1 (P < 0.001).

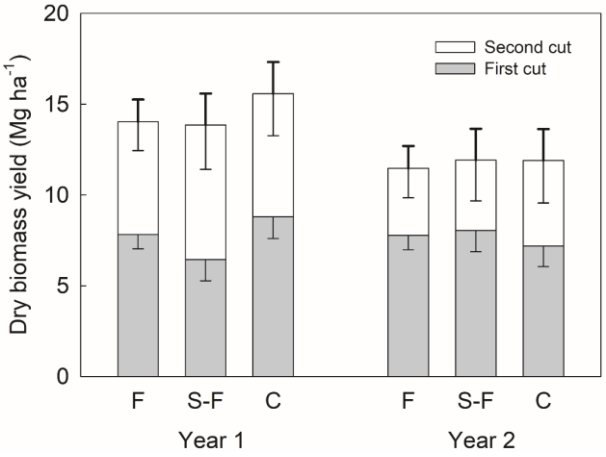

Figure 6. Mean aboveground biomass yields in the two study years from flooded (F), semi-flooded (S-F) and control (C) plots. Total bar heights denote the combined annual yield of the respective first and second cuts. Error bars represent one side of the 95 % confidence intervals (n = 8 for F plots and n = 4 for S-F and C plots). Thin downward error bars represent errors for individual cuts and thick upward error bars represent errors for total yield.

Dynamics of mid-day CO_2 fluxes

The mid-day NEE followed a seasonal pattern with large net CO_2 uptake during growing periods, which decreased and remained close to zero during the non-growing periods (Figure 5d). NEE was similar in all treatments during the first cut periods in both years. However, as the regrowth of biomass was delayed in the flooded plots after the first harvest, particularly in Year 2, the net uptake of CO_2 was weaker during that period. The NEE fluxes in non-growing periods were small but mostly negative, as the plots contained green biomass after the final harvest in autumn and soil respiration was restricted due to flooded field conditions.

The mid-day ER followed a strong seasonal trend (Figure 5e) and correlated well with air temperature (mean r = 0.82; range 0.79–0.86 for individual collars), RVI (mean r = 0.84; range 0.81–0.86) and WTD (mean r = 0.49; range 0.23–0.67 for individual collars in semi-flooded and control plots). This indicated that temperature, green biomass (Figure 5a,c) and water table (Figure 4c) were the major driving factors for seasonal variations in ER. During the growing periods, ER in the flooded plots was consistently lower than in the semi-flooded and control plots. However, ER was similar in all treatments during the non-growing periods in accordance with similar WTD and RVI.

Mid-day GPP showed a clear correlation to PAR (mean r = 0.82; range 0.76–0.87 for individual collars) and RVI (mean r = 0.58; range 0.52–0.61), thus following a seasonal trend and responding to harvest events (Figure 5). Dynamics of GPP at all WTD treatments were generally similar but absolute GPP was lower in the flooded plots after the first harvest, particularly in Year 2 (Figure 5f).

Comparative CO_2 flux modelling

Model performance and model selection

Among the models for ER, the NSE across the treatments was 0.63–0.75 for models with temperature as the only predictor (Models 1 and 2), indicating good statistical performance (Tables A1–A3 in the Appendix). Yet NSE was higher (0.77–0.88) for models with both temperature and RVI as predictors (Models 3–8), indicating very good statistical performance. Also, the consistency of NSE across WTD treatments was higher for Models 3–8 than for Models 1 and 2.

Among the GPP models that included PAR and RVI (Models 2–8), the NSE across the treatments was 0.82–0.92 (Tables A4–A6), i.e., indicating very good to excellent statistical performance. For GPP Model 1 (without RVI), NSE at individual campaigns mostly ranged from 0.44 to 0.99, except on a few occasions (< 5 %) where the modelled light response curves had lower NSE, i.e., after harvest and in winter. The average NSE for GPP Model 1 was 0.80.

 DOI: 10.19189/MaP.2017.DW.322

Although comparative flux modelling highlighted RVI as a useful variable in the ER and GPP model structures, it did not allow rigorous selection among the relevant models due to rather similar NSE values. Further model evaluation based on Akaikes Information Criterion (AIC) and adjusted R^2 resulted in similar conclusions (data not shown). However, model validation using simultaneous *F*-test for unit slope and zero intercept indicated a bias ($P < 0.05$) for ER Models 3 and 6 for flooded treatments (Tables A1–A3) and also for GPP Models 2, 4 and 6 for all treatments (Tables A4–A6). The combination of higher NSE and non-significant *P*-value for the *F*-test indicated that ER Model 4 was the most suitable model for flooded treatments and ER Models 4, 5 and 6 were equally suitable models for semi-flooded and control treatments. As Model 4 was generally better for all treatments, this model was selected for further collar-scale assessment of WTD treatment effects on annual ER. For GPP, Models 3, 5 and 7 performed the best and equally well for all treatments. However, Model 5 without temperature scaling (FT) was not used as it did not account for the effect of low temperature on photosynthesis. Model 7 with marginally higher NSE than Model 3 across all treatments was selected for further assessment of WTD treatment effects on annual GPP for each collar.

Annual estimates and CO_2 emission factors in relation to modelling uncertainty

The mean and range of annual ER (expressed as CO_2-C; g m^{-2} $year^{-1}$) estimated with the eight models for flooded, semi-flooded and control plots were 1128 ± 20 %, 1402 ± 21 % and 1496 ± 22 %, respectively, in Year 1 and 1079 ± 19 %, 1418 ± 15 % and 1490 ± 14 %, respectively, in Year 2 (Figure 7a,b). The lowest annual ER estimates were generally derived from Models 1 and 2 (without RVI) and 6, whereas

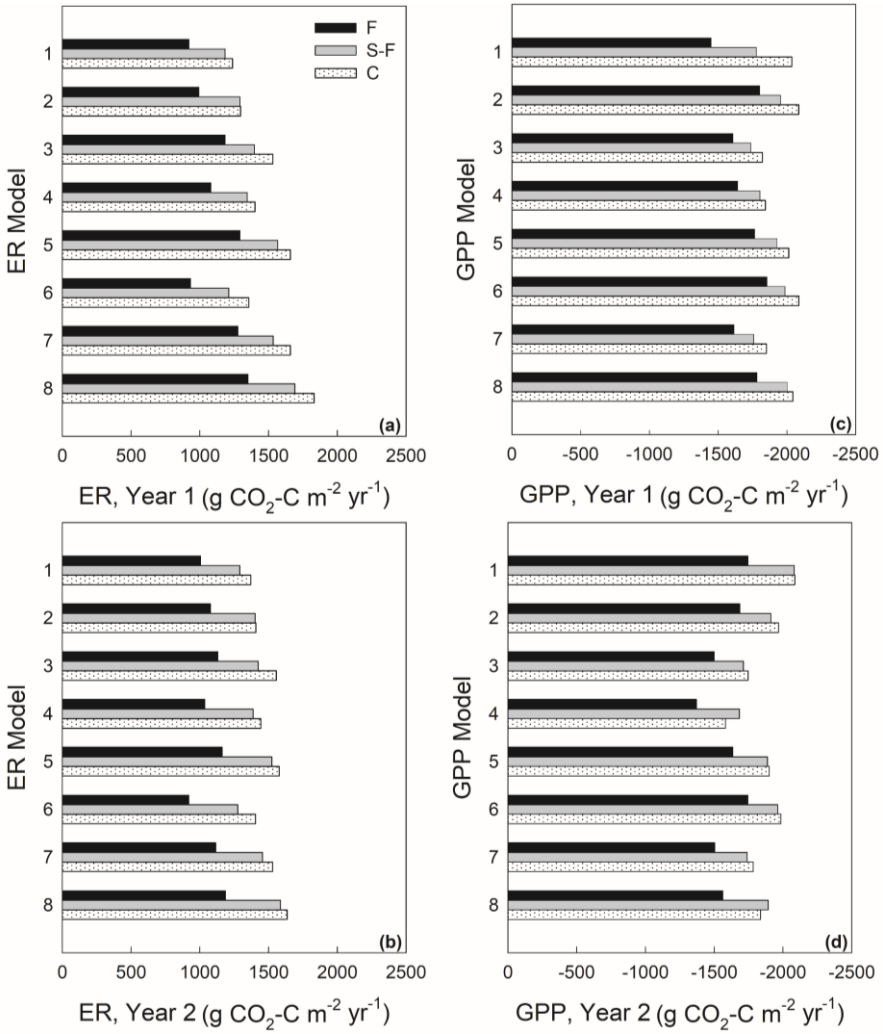

Figure 7. (a, b) Annual ecosystem respiration (ER) and (c, d) annual gross primary production (GPP) estimates with different ER and GPP models (see Tables 1 and 2) at the different WTD treatments, i.e., flooded (F), semi-flooded (S-F) and control (C). Data are shown for each study year.

the highest estimates were derived from Model 8. Despite the differences in absolute ER values, all models showed a consistent pattern of WTD treatment effects where ER increased from flooded to semi-flooded to control treatments (Figure 7a,b).

Annual GPP (g CO_2-C m^{-2} $year^{-1}$; numerical values) estimated with the eight models for flooded, semi-flooded and control plots were 1704 ± 12 %, 1869 ± 11 % and 1973 ± 10 %, respectively, in Year 1 and 1594 ± 14 %, 1859 ± 11 % and 1862 ± 15 %, respectively, in Year 2 (Figure 7c,d). For all individual GPP models (and years) it was found that CO_2 uptake generally increased from flooded to semi-flooded to control management (Figure 7c,d).

Although treatment effects on ER and GPP were robust among the different models, the resulting outcome for annual NEE was highly uncertain due to NEE being the (small) difference between two large component fluxes (Figure 8). Thus, the 64 possible NEE combinations (from the eight ER and eight GPP estimates) led to different but negative NEE depending on model selection, yet with two combinations indicating control treatments as weak sources of CO_2. CO_2 emission factors varied between

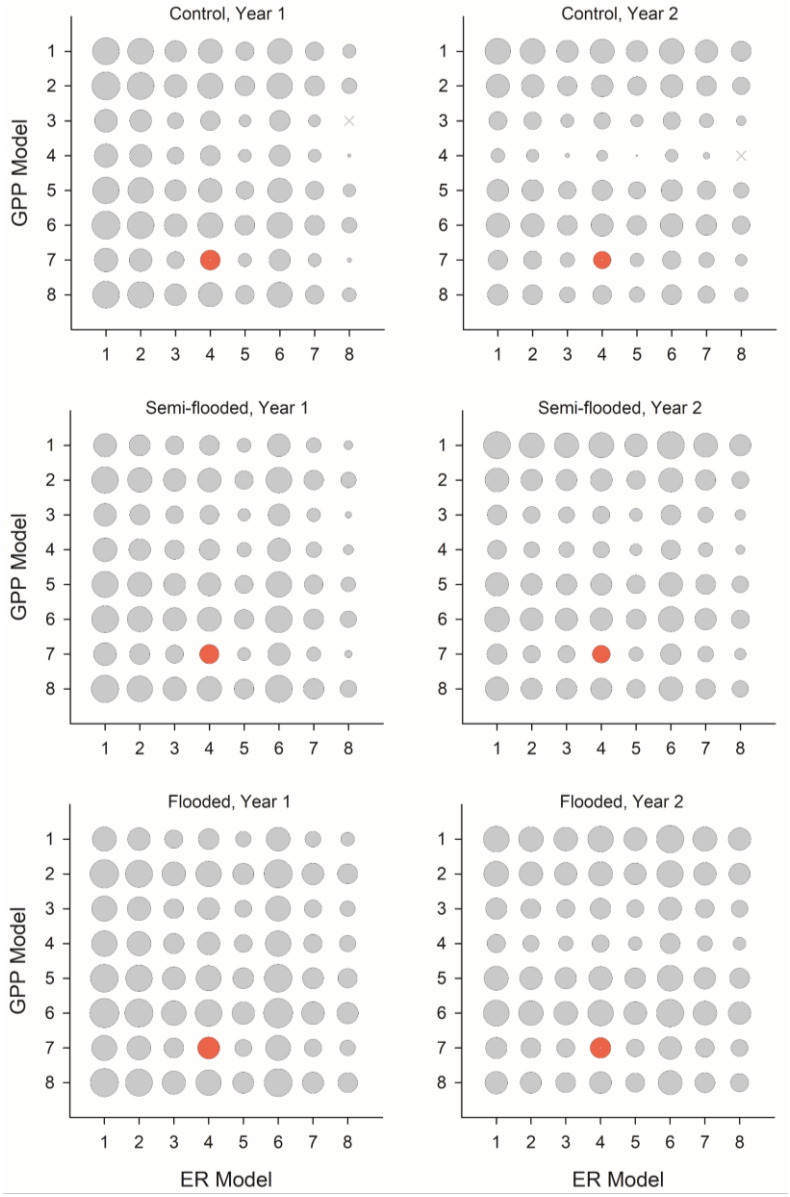

Figure 8. Bubble plot of resulting net ecosystem exchange (NEE) of CO_2 derived by combining the eight times eight ecosystem respiration (ER) and gross primary production (GPP) models (as depicted in Tables 1 and 2) for individual treatments and study years. Maximum symbol size corresponds to a NEE sink strength of - 935 g CO_2-C m^{-2} $year^{-1}$. Red symbols show the resulting NEE from the two selected models, ER Model 4 and GPP Model 7. Crosses show incidences of small positive NEE fluxes.

strong sink and source of CO_2, depending on model selection (Figure 9). However, more frequent indication of sinks of CO_2 (negative emission factor) was observed for flooded treatments.

Annual CO_2 emissions in relation to WTD treatments

The two selected models, ER Model 4 and GPP Model 7, were individually run for each collar and showed a significant effect of WTD treatment on both ER ($P < 0.001$) and GPP ($P = 0.003$) (Figure 10). Annual ER increased significantly in Year 2 except for the flooded treatment ($P = 0.003$), whereas annual GPP decreased significantly in Year 2 ($P < 0.001$) in all treatments. There was no significant effect of WTD treatment on annual NEE ($P = 0.069$). However, annual NEE was significantly lower in Year 2 as compared to Year 1 ($P < 0.001$). There were no significant effects of year ($P = 0.094$) and WTD treatment ($P = 0.105$) on the annual CO_2 emission factors.

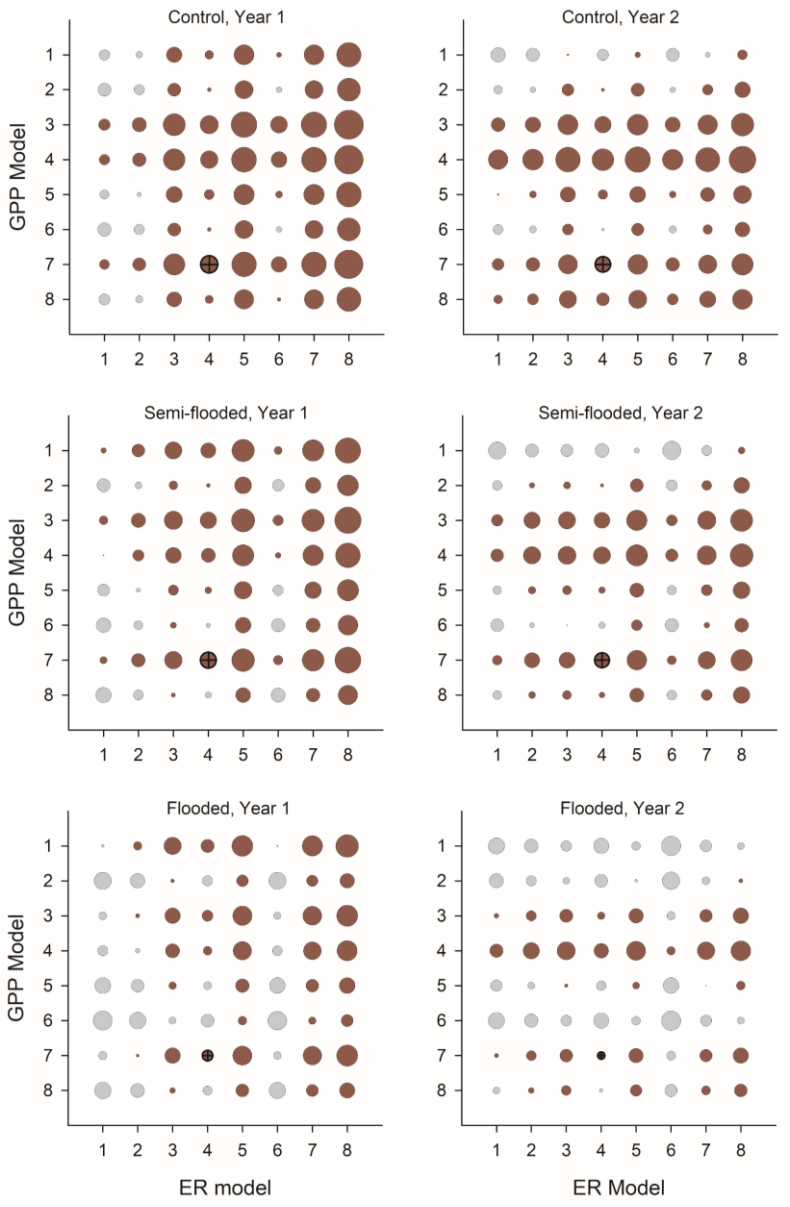

Figure 9. Bubble plot of resulting emission factors of CO_2 derived from net ecosystem exchange (NEE) of CO_2 and biomass yield C export for individual treatments and study years. NEE of CO_2 was derived by combining the eight times eight ecosystem respiration (ER) and gross primary production (GPP) models (as depicted in Tables 1 and 2). Maximum symbol size corresponds to numerical emission factors of 709 g CO_2-C m^{-2} $year^{-1}$. Grey symbols indicate negative emissions (sink of CO_2); maroon symbols show positive emissions (source of CO_2). Maroon symbols with cross show the resulting CO_2 emission factor from the two selected models, ER Model 4 and GPP Model 7.

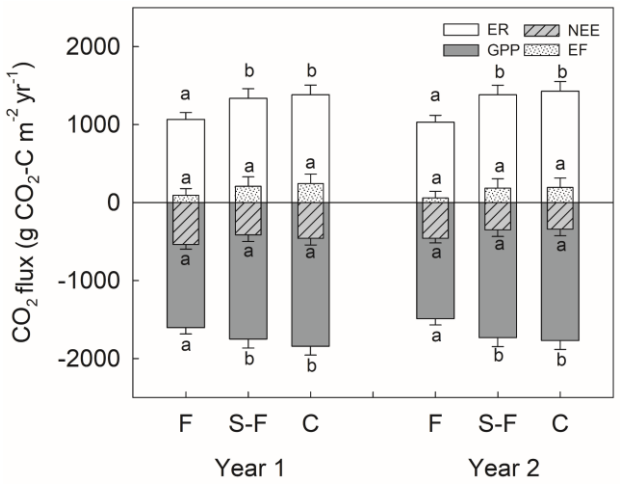

Figure 10. Annual budgets of ecosystem respiration (ER), gross primary production (GPP), net ecosystem exchange (NEE) and CO_2 emission factor (EF; calculated as the sum of NEE and carbon exported in harvested biomass). Data are shown for flooded (F), semi-flooded (S-F) and control (C) plots. Error bars represent the upper 95 % confidence interval (n = 8 for F plots, n = 4 for S-F and C plots). Treatments marked with different letters denotes significant differences within each year ($P < 0.05$).

DISCUSSION

The two-year field study was designed to compare CO_2 fluxes from side-by-side rewetted and drained (control) plots cultivated with perennial grasses. However, as both study years were wetter than the long-term average, differences in WTD among the treatments were less than expected, and hence CO_2 fluxes were studied at scenarios of rather shallow water table corresponding to (two-year) weighted mean WTDs of 1, 3 and 9 cm below the soil surface for flooded, semi-flooded and control plots, respectively. Therefore, the annual average WTD in the control plots (9 cm) was much shallower than observed previously in the same site (40 cm; Karki *et al.* 2015a). This may, to some extent, also be related to the gradually deteriorating maintenance of the drainage system at the study site.

Biomass yield

Total annual biomass yields (11–16 Mg DM ha^{-1}) obtained in this study were within the range observed under similar intensive management of perennial grasses in field and mesocosm studies (Kandel *et al.* 2013a, Karki *et al.* 2016). In Year 2, plant growth was restricted due to higher water table after the first cut, which contributed to significantly lower biomass yield. Compared to Year 1, the site received 90 mm more precipitation during the month following first harvest in Year 2, which caused flooding at most of the plots. After the summer harvests, the stubble remained below the water surface for extended periods in the flooded and semi-flooded plots, which delayed regrowth of the plants. As observed in this study, Fraser & Karnezis (2005) also reported dieback of flood-tolerant grasses including RCG when the plants were submerged. This indicates that the perennial grasses under paludiculture should be harvested to ensure that stubble height is above the flooding level.

Model selection

Model validation is important for model selection but can be done with several approaches each with specific justifications (Haefner 2005). Validation and selection based on NSE indicated that several of the tested models could qualify for extrapolation of the CO_2 fluxes to annual estimates. However, analysis of modelled versus measured CO_2 fluxes by simultaneous *F*-test for unit slope and zero intercept indicated potential bias for some models even with high NSE. Also, ER Model 7 had a higher NSE, but predicted negative ER when the temperature was below zero, which is biologically incorrect.

In the present study, temperature and RVI were included as driving factors for ER. However, ER is also affected by WTD, and it is common to include WTD in the model structure to achieve a better prediction of ER (Rowson *et al.* 2013, Karki *et al.* 2014, Kandel *et al.* 2018). In the present study, the effect of including WTD was tentatively tested for the selected ER model (Model 4) as suggested by Karki *et al.* (2014), using hourly values of WTD as reconstructed from linear interpolation between measurement days (data not shown). However, the inclusion of WTD for analyses of ER did not lead to an improvement for the flooded plots (where WTD was rather constant during the entire measurement period) and including WTD only improved model performance slightly for the semi-flooded and control plots with an increase in NSE from 0.88 to 0.92 and from 0.82 to 0.85, respectively. Furthermore, there were only minor differences in annual ER estimates (< 5 %) derived from models with and without WTD (data not shown).

Model 1 for GPP is the most commonly used model for annual estimations of GPP (Elsgaard *et al.* 2012, Beetz *et al.* 2013, Minke *et al.* 2016). However, this approach requires that models are run for each measurement campaign, and it poorly captures temporal variability especially under field conditions with management interventions such as harvest

 DOI: 10.19189/MaP.2017.DW.322

(Görres *et al.* 2014). The use of GPP models that include RVI (or other vegetation indices) can provide more robust methods for capturing such temporal variations (Wohlfahrt *et al.* 2010, Kandel *et al.* 2013b; Kandel *et al.* 2017). In addition, such models can be analysed in one single run integrating information obtained from the entire study period. A temperature modifier function (FT) was included in several models to adjust for low temperature constraints on photosynthesis (Kandel *et al.* 2017). The importance of including FT was seen, for example, with GPP Model 3 where it corrected the bias observed without the FT function (Model 2).

Uncertainties in CO_2 fluxes from rewetted peatlands, recognised in IPCC Tier 1 emission factors, are already considerable due to variations in variables such as peat type (fen or bog), nutrient status, vegetation, hydrology, number of years after rewetting, previous land use and climate (Wilson *et al.* 2016a). In addition, the use of different measurement and gap filling strategies leads to further uncertainty in annual fluxes (Huth *et al.* 2017). Our results indicate that the selection of response models for ER and GPP strongly contributes to uncertainties and substantiates the importance of working towards unified and comparable approaches for modelling CO_2 fluxes from chamber measurements (Huth *et al.* 2017). Although we found that individual ER and GPP models provided a consistent pattern in relation to WTD treatment effects, arbitrary combinations of the two component fluxes into NEE resulted in a wide range of outcomes.

Annual CO_2 budgets

The annual ER in the control plots in Year 1 obtained with Model 6 (1356 g CO_2-C m^{-2}) was similar to the annual ER in a concurrent study at the same site where festulolium (fescue-ryegrass hybrid) and tall fescue were cultivated under a two-cut management system (1368 g CO_2-C m^{-2}) when analysed by the same model (Kandel *et al.* 2017). The annual ER was significantly lower from the flooded plots than the semi-flooded and control plots, despite the small difference in annual WTD. According to Chimner & Cooper (2003) and Riutta *et al.* (2007), most of the easily oxidised labile C is present near the soil surface (the upper 0–15 cm) and exposing this zone to anaerobic conditions can significantly reduce soil respiration. Moreover, plant respiration may also be lowered in flooded plots due to decreased GPP (Karki *et al.* 2015b, Järveoja *et al.* 2016). The strong correlation between all measured GPP at 100 % PAR and ER (r = 0.85, P < 0.001) underlined the importance of plant respiration for total ER.

An effect of WTD management on GPP in peatlands has been frequently observed, substantiated by changes in biomass yield and composition (Riutta *et al.* 2007, Waddington *et al.* 2010, Järveoja *et al.* 2016, Laine *et al.* 2016). In the present study, neither the biomass yield nor the biomass composition was significantly different among the WTD treatments. The biomass was mainly composed of RCG and *Poa* spp. in all plots. In this study, reduced GPP in the flooded plots was mostly due to restriction of plant growth for the extended period after the first cut because of higher water table.

In a meta-analysis, Wilson *et al.* (2016a) reported that net uptake of CO_2 increased linearly with decreasing WTD for a gradient from 30 cm below to 20 cm above the soil surface. In this study, where the annual WTD varied within a narrow range between treatments, no significant effect of WTD on annual NEE could be registered. In the current study, smaller WTD reduced both ER and GPP thus counterbalancing the effect on NEE as reported by Järveoja *et al.* (2016). Inter-annual variability in NEE from peatlands is often seen due to high sensitivity to prevailing weather conditions (Herbst *et al.* 2013, Helfter *et al.* 2015, Wilson *et al.* 2016b). Indeed, both study years were wetter than long-term average, so potential interactions between WTD treatments and more dry weather conditions could not be assessed. The range of annual NEE values obtained in this study was generally at the lower range (higher net CO_2 uptake) of NEE previously reported from diverse rewetted fen peatlands (IPCC 2014, Minke *et al.* 2016, Wilson *et al.* 2016a). However, relatively similar low NEE has been observed in rewetted peatlands with productive species like RCG and *Typha latifolia* (Wilson *et al.* 2007), *Phragmites australis* (Minke *et al.* 2016) and *Eriophorum angustifolium* (Wilson *et al.* 2013). Yet, direct comparison of annual fluxes with other studies is difficult as it partly depends on the methods used to estimate annual emissions.

CO_2 emission factors

CO_2 emission factors ranged from 0.6 to 2.4 Mg CO_2-C ha^{-1} yr^{-1} which fall within or slightly above the 95 % confidence interval (-0.71 to 1.71 Mg CO_2-C ha^{-1} yr^{-1}) of emission factors for rewetted nutrient rich temperate fens proposed by the IPCC (2014). Nevertheless, similar emission factors of up to 2.1 Mg CO_2-C ha^{-1} yr^{-1} have been reported from rewetted peatlands where biomass was removed by grazing (Renou-Wilson *et al.* 2016). The CO_2 emission factors obtained in this study were substantially lower than the emission factors (6–12 Mg CO_2-C ha^{-1} yr^{-1}) reported for deeper

 DOI: 10.19189/MaP.2017.DW.322

drained peatlands in Denmark (Elsgaard *et al*. 2012, Kandel *et al*. 2013b) supporting the conclusion that rewetting and biomass cultivation can amply reduce CO_2 losses from drained peatlands (Gunther *et al*. 2015, Karki *et al*. 2016). This is despite the fact that biomass yield was optimised by intensive management, such as multiple harvesting and fertilisation. Yet, in comparing CO_2 emission factors among rewetted and drained peatlands, the role of methane (CH_4) emissions for the C balance at rewetted sites should also be considered. Rewetting and subsequent colonisation by wetland plants may generally increase the CH_4 emissions (Gunther *et al.* 2015, Harpenslager *et al.* 2015, Vanselow-Algan *et al* 2015, Karki *et al*. 2016).

In conclusion, this field study showed significant differences in both annual ER and GPP despite a small difference in WTD treatments with two-year annual means of 1, 3 and 9 cm below the soil surface. The choice of response models for annual estimations of flux measurements contributed to uncertainties in estimates of ER and GPP. However, the WTD treatment effects were generally robust among the different response models. There was no significant difference in NEE and CO_2 emission factors (the sum of NEE and carbon export in harvested biomass) among the shallow WTD treatments (annual means, < 10 cm below the soil surface). However, the effects of other factors such as changes in vegetation composition and inter-annual climate variability may need to be addressed on a longer time scale than achieved in the present study, which was restricted to the first two years following rewetting.

ACKNOWLEDGEMENTS

The study was financially supported by the Innovation Fund Denmark under the EU FACCE ERA-NET+ on Climate Smart Agriculture as a part of the CAOS project (www.caos-project.eu) and the PEATWISE project (http://eragas.eu/index.php/research-projects/peatwise) in the frame of the ERA-NET FACCE ERA-GAS. FACCE ERA-GAS has received funding from the European Union's Horizon 2020 research and innovation program under Grant Agreement No. 696356. The authors would like to express their gratitude for assistance provided by Jens B. Kjeldsen and the team of technicians in crop management and harvesting at AU-Foulumgård. We also wish to acknowledge the skilled technical assistance of Ahammad Mostafa Kamal, Bodil Stensgaard, Ben McCarthy, Henrik Nørgaard, Michael Koppelgaard, Morten Skov and Suman Thapa. This article is based on a presentation at the international conference *Renewable Resources from Wet and Rewetted Peatlands* held on 26–28 September 2017 at the University of Greifswald, Germany. We thank the two anonymous referees and David Wilson for their comments which helped us to improve the manuscript.

REFERENCES

Al-Shooshan, A.A. (1997) Estimation of photosynthetically active radiation under an arid climate. *Journal of Agricultural Engineering Research*, 66, 9–13.

Beetz, S., Liebersbach, H., Glatzel, S., Jurasinski, G., Buczko, U. & Höper, H. (2013) Effects of land use intensity on the full greenhouse gas balance in an Atlantic peat bog. *Biogeosciences*, 10, 1067–1082.

Benjamini, Y. & Hochberg, Y. (1995) Controlling the false discovery rate: a practical and powerful approach to multiple testing. *Journal of the Royal Statistical Society. Series B (Methodological)*, 57, 289–300.

Benjamini, Y. & Yekutieli, D. (2001) The control of the false discovery rate in multiple testing under dependency. *The Annals of Statistics*, 29, 1165–1188.

Biancalani, R. & Avagyan, A. (2014) *Towards Climate-Responsible Peatlands Management*. Mitigation of Climate Change in Agriculture Series (MICCA) 9, Food and Argiculture Organization of the United Nations, Rome, 100 pp.

Chimner, R.A. & Cooper, D.J. (2003) Influence of water table levels on CO_2 emissions in a Colorado subalpine fen: an in situ microcosm study. *Soil Biology and Biochemistry*, 35, 345–351.

Dinsmore, K.J., Skiba, U.M., Billett, M.F. & Rees, R.M. (2009) Effect of water table on greenhouse gas emissions from peatland mesocosms. *Plant and Soil*, 318, 229–242.

Elsgaard, L., Görres, C.-M., Hoffmann, C.C., Blicher-Mathiesen, G., Schelde, K. & Petersen, S.O. (2012) Net ecosystem exchange of CO_2 and carbon balance for eight temperate organic soils under agricultural management. *Agriculture, Ecosystems & Environment*, 162, 52–67.

Fraser, L.H. & Karnezis, J.P. (2005) A comparative assessement of seedling survival and biomass accumulation for fourteen wetland plant species grown under minor water-depth differences. *Wetlands*, 25, 520–530.

Gorham, E. (1991) Northern peatlands: role in the carbon cycle and probable responses to climatic warming. *Ecological Applications*, 1, 182–195.

Görres, C.-M., Kutzbach, L. & Elsgaard, L. (2014)

 DOI: 10.19189/MaP.2017.DW.322

Comparative modeling of annual CO_2 flux of temperate peat soils under permanent grassland management. *Agriculture, Ecosystems & Environment*, 186, 64–76.

Günther, A., Huth, V., Jurasinski, G. & Glatzel, S. (2015) The effect of biomass harvesting on greenhouse gas emissions from a rewetted temperate fen. *GCB Bioenergy*, 7, 1092–1106.

Haefner, J.W. (2005) *Modelling Biological Systems: Principles and Application*. Second edition, Springer, New York, 475 pp.

Harpenslager, S.F., van den Elzen, E., Kox, M.A.R., Smolders, A.J.P., Ettwig, K.F. & Lamers, L.P.M. (2015) Rewetting former agricultural peatlands: Topsoil removal as a prerequisite to avoid strong nutrient and greenhouse gas emissions. *Ecological Engineering*, 84, 159–168.

Helfter, C., Campbell, C., Dinsmore, K.J., Drewer, J., Coyle, M., Anderson, M., Skiba, U., Nemitz, E., Billett, M.F. & Sutton, M.A. (2015) Drivers of long-term variability in CO_2 net ecosystem exchange in a temperate peatland. *Biogeosciences*, 12, 1799–1811.

Herbst, M., Friborg, T., Schelde, K., Jensen, R., Ringgaard, R., Vasquez, V., Thomsen, A.G. & Soegaard, H. (2013) Climate and site management as driving factors for the atmospheric greenhouse gas exchange of a restored wetland. *Biogeosciences*, 10, 39–52.

Hoffmann, M., Jurisch, N., Borraz, E.A., Hagemann, U., Drösler, M., Sommer, M. & Augustin, J. (2015) Automated modeling of ecosystem CO_2 fluxes based on periodic closed chamber measurements: a standardized conceptual and practical approach. *Agricultural and Forest Meteorology*, 200, 30-45.

Hooijer, A., Page, S., Jauhiainen, J., Lee, W.A., Lu, X.X., Idris, A. & Anshari, G. (2012) Subsidence and carbon loss in drained tropical peatlands. *Biogeosciences*, 9, 1053–1071.

Huth, V., Vaidya, S., Hoffmann, M., Jurisch, N., Günther, A., Gundlach, L., Hagemann, U., Elsgaard, L. & Augustin, J. (2017) Divergent NEE balances from manual-chamber CO_2 fluxes linked to different measurement and gap-filling strategies: A source for uncertainty of estimated terrestrial C sources and sinks? *Journal of Plant Nutrition and Soil Science*, 180, 302–315.

IPCC (2014) *2013 Supplement to the 2006 IPCC Guidelines for National Greenhouse Gas Inventories: Wetlands*, Hiraishi, T., Krug, T., Tanabe, K., Srivastava, N., Baasansuren, J., Fukuda, M. & Troxler, T.G. (eds.). IPCC, Switzerland, 354 pp. Online at: https://www. ipcc-nggip.iges.or.jp/public/ wetlands/, accessed 15 Mar 2019.

Järveoja, J., Peichl, M., Maddison, M., Soosaar, K., Vellak, K., Karofeld, E., Teemusk, A. & Mander, Ü. (2016) Impact of water table level on annual carbon and greenhouse gas balances of a restored peat extraction area. *Biogeosciences*, 13, 2637–2651.

Joosten, H., Gaudig, G., Krawczynski, R., Tanneberger, F., Wichmann, S. & Wichtmann, W. (2015) Managing soil carbon in Europe: Paludicultures as a new perspective for peatlands. In: Banwart, S.A., Noellemeyer, E. & Milne, E. (eds.) *Soil Carbon: Science, Management and Policy for Multiple Benefits*, CABI International, Wallingford, UK and Boston, USA, 297–306.

Kandel, T.P., Elsgaard, L., Karki, S. & Lærke, P.E. (2013a) Biomass yield and greenhouse gas emissions from a drained fen peatland cultivated with reed canary grass under different harvest and fertilizer regimes. *BioEnergy Research*, 6, 883–895.

Kandel, T.P., Elsgaard, L. & Lærke, P.E. (2013b) Measurement and modelling of CO_2 flux from a drained fen peatland cultivated with reed canary grass and spring barley. *GCB Bioenergy*, 5, 548–561.

Kandel, T.P., Sutaryo, S., Møller, H.B., Jørgensen, U. & Lærke, P.E. (2013c) Chemical composition and methane yield of reed canary grass as influenced by harvesting time and harvest frequency. *Bioresource Technology*, 130, 659–666.

Kandel, T.P., Lærke, P.E. & Elsgaard, L. (2016) Effect of chamber enclosure time on soil respiration flux: A comparison of linear and non-linear flux calculation methods. *Atmospheric Environment*, 141, 245–254.

Kandel, T.P., Elsgaard, L. & Lærke, P.E. (2017) Annual balances and extended seasonal modelling of carbon fluxes from a temperate fen cropped to festulolium and tall fescue under two-cut and three-cut harvesting regimes. *GCB Bioenergy*, 9, 1690–1706.

Kandel, T.P., Lærke, P.E. & Elsgaard, L. (2018) Annual emissions of CO_2, CH_4 and N_2O from a temperate peat bog: Comparison of an undrained and four drained sites under permanent grass and arable crop rotations with cereals and potato. *Agricultural and Forest Meteorology*, 256–257, 470–481.

Kandel, T.P., Lærke, P.E., Hoffmann, C.C. & Elsgaard, L. (2019) Complete annual CO_2, CH_4, and N_2O balance of a temperate riparian wetland 12 years after rewetting. *Ecological Engineering*, 127, 527–535.

Karki, S., Elsgaard, L., Audet, J. & Lærke, P. (2014) Mitigation of greenhouse gas emissions from reed

 DOI: 10.19189/MaP.2017.DW.322

canary grass in paludiculture: effect of groundwater level. *Plant and Soil*, 383, 217–230.

Karki, S., Elsgaard, L., Kandel, T.P. & Lærke, P.E. (2015a) Full GHG balance of a drained fen peatland cropped to spring barley and reed canary grass using comparative assessment of CO_2 fluxes. *Environmental Monitoring and Assessment*, 187, 62–75.

Karki, S., Elsgaard, L. & Lærke, P.E. (2015b) Effect of reed canary grass cultivation on greenhouse gas emission from peat soil at controlled rewetting. *Biogeosciences*, 12, 595–606.

Karki, S., Elsgaard, L., Kandel, T.P. & Lærke, P.E. (2016) Carbon balance of rewetted and drained peat soils used for biomass production: a mesocosm study. *GCB Bioenergy*, 8, 969–980.

Kløve, B., Berglund, K., Berglund, Ö., Weldon, S. & Maljanen, M. (2017) Future options for cultivated Nordic peat soils: Can land management and rewetting control greenhouse gas emissions? *Environmental Science & Policy*, 69, 85–93.

Knadel, M., Thomsen, A. & Greve, M.H. (2011) Multisensor on-the-go mapping of soil organic carbon content. *Soil Science Society of America Journal*, 75, 1799–1806.

Kutzbach, L., Schneider, J., Sachs, T., Giebels, M., Nykänen, H., Shurpali, N.J., Martikainen, P.J., Alm, J. & Wilmking, M. (2007) CO_2 flux determination by closed-chamber methods can be seriously biased by inappropriate application of linear regression. *Biogeosciences*, 4, 1005–1025.

Labouriau, R. (2018) Applied Statistical Laboratory: pairwise comaparisons. Online at: http://home.math.au.dk/rodrigo/astatlab/software/pairwisecomparisons/, accessed 09 May 2018.

Laine, A.M., Tolvanen, A., Mehtätalo, L. & Tuittila, E-S. (2016) Vegetation structure and photosynthesis respond rapidly to restoration in young coastal fens. *Ecology and Evolution*, 6, 6880–6891.

Leifeld, J., Müller, M. & Fuhrer, J. (2011) Peatland subsidence and carbon loss from drained temperate fens. *Soil Use and Management*, 27, 170–176.

Lloyd, J. & Taylor, J.A. (1994) On the temperature dependence of soil respiration. *Functional Ecology*, 8, 315–323.

Mäkiranta, P., Riutta, T., Penttilä, T. & Minkkinen, K. (2010) Dynamics of net ecosystem CO_2 exchange and heterotrophic soil respiration following clearfelling in a drained peatland forest. *Agricultural and Forest Meteorology*, 150, 1585–1596.

Minke, M., Augustin, J., Burlo, A., Yarmashuk, T., Chuvashova, H., Thiele, A., Freibauer, A., Tikhonov, V. & Hoffmann, M. (2016) Water level, vegetation composition, and plant productivity explain greenhouse gas fluxes in temperate cutover fens after inundation. *Biogeosciences*, 13, 3945–3970.

Moldrup, P., Olesen, T., Schjønning, P., Yamaguchi, T. & Rolston, D.E. (2000) Predicting the gas diffusion coefficient in undisturbed soil from soil water characteristics. *Soil Science Society of America Journal*, 64, 94–100.

Nash, J.E. & Sutcliffe, J.V. (1970) River flow forecasting through conceptual models part I — A discussion of principles. *Journal of Hydrology*, 10, 282–290.

Piñeiro, G., Perelman, S., Guerschman, J.P. & Paruelo, J.M. (2008) How to evaluate models: Observed vs. predicted or predicted vs. observed? *Ecological Modelling*, 216, 316–322.

Plauborg, F., Iversen, B.V. & Lærke, P.E. (2005) In situ comparison of three dielectric soil moisture sensors in drip irrigated sandy soils. *Vadose Zone Journal*, 4, 1037–1047.

Poyda, A., Reinsch, T., Kluß, C., Loges, R. & Taube, F. (2016) Greenhouse gas emissions from fen soils used for forage production in northern Germany. *Biogeosciences*, 13, 5221–5244.

R Core Team (2016) *R: A Language and Environment for Statistical Computing*. R Foundation for Statistical Computing, Vienna, Austria. Online at: https://www.r-project.org/

Renou-Wilson, F., Barry, C., Müller, C. & Wilson, D. (2014) The impacts of drainage, nutrient status and management practice on the full carbon balance of grasslands on organic soils in a maritime temperate zone. *Biogeosciences*, 11, 4361–4379.

Renou-Wilson, F., Müller, C., Moser, G. & Wilson, D. (2016) To graze or not to graze? Four years greenhouse gas balances and vegetation composition from a drained and a rewetted organic soil under grassland. *Agriculture, Ecosystems & Environment*, 222, 156–170.

Riutta, T., Laine, J. & Tuittila, E.-S. (2007) Sensitivity of CO_2 exchange of fen ecosystem components to water level variation. *Ecosystems*, 10, 718–733.

Rowson, J.G., Worrall, F. & Evans, M.G. (2013) Predicting soil respiration from peatlands. *Science of the Total Environment*, 442, 397–404.

Shrestha, J., Niklaus, P.A., Pasquale, N., Huber, B., Barnard, R.L., Frossard, E., Schleppi, P., Tockner, K. & Luster, J. (2014) Flood pulses control soil nitrogen cycling in a dynamic river floodplain. *Geoderma*, 228–229, 14–24.

Soini, P., Riutta, T., Yli-Petäys, M. & Vasander, H. (2010) Comparison of vegetation and CO_2 dynamics between a restored cut-away peatland

 DOI: 10.19189/MaP.2017.DW.322

and a pristine fen: Evaluation of the restoration success. *Restoration Ecology*, 18, 894–903.

Thornley, J.H. & Johnson, I.R. (1990) *Plant and Crop Modelling: A Mathematical Approach to Plant and Crop Physiology*. Clarendon Press, Fairlawn NJ, 73 pp.

Tiemeyer, B., Albiac Borraz, E., Augustin, J., Bechtold, M., Beetz, S., Beyer, C., Drösler, M., Ebli, M., Eickenscheidt, T., Fiedler, S., Förster, C., Freibauer, A., Giebels, M., Glatzel, S., Heinichen, J., Hoffmann, M., Höper, H., Jurasinski, G., Leiber-Sauheitl, K., Peichl-Brak, M., Roßkopf, N., Sommer, M. & Zeitz, J. (2016) High emissions of greenhouse gases from grasslands on peat and other organic soils. *Global Change Biology*, 22, 4134–4149.

Tubiello, F.N., Biancalani, R., Salvatore, M., Rossi, S. & Conchedda, G. (2016) A worldwide assessment of greenhouse gas emissions from drained organic soils. *Sustainability*, 8, 371–384.

Urbanová, Z., Picek, T. & Tuittila, E.-S. (2013) Sensitivity of carbon gas fluxes to weather variability on pristine, drained and rewetted temperate bogs. *Mires and Peat*, 11(04), 1–14.

Vanselow-Algan, M., Schmidt, S.R., Greven, M., Fiencke, C., Kutzbach, L. & Pfeiffer, E.M. (2015) High methane emissions dominate annual greenhouse gas balances 30 years after bog rewetting. *Biogeosciences*, 12, 4361–4371.

Waddington, J.M., Strack, M. & Greenwood, M.J. (2010) Toward restoring the net carbon sink function of degraded peatlands: Short-term response in CO_2 exchange to ecosystem-scale restoration. *Journal of Geophysical Research: Biogeosciences*, 115, G01008, 1–13.

Walpersdorf, E., Koch, C.B., Heiberg, L., O'Connell, D.W., Kjaergaard, C. & Hansen, H.C.B. (2013) Does vivianite control phosphate solubility in anoxic meadow soils? *Geoderma*, 193–194, 189–199.

Wichtmann, W., Schröder, C. & Joosten, H. (2016) *Paludiculture - Productive Use of Wet Peatlands. Climate Protection – Biodiversity - Regional Economic Benefits*. Schweizerbart Science Publishers, Stuttgart; Germany, 272 pp.

Wiegand, C.L. & Richardson, A.J. (1984) Leaf area, light interception and yield estimates from spectral components analysis. *Agronomy Journal*, 76, 543–548.

Wilson, D., Tuittila, E-S., Alm, J., Laine, J., Farrell, E.P. & Byrne, K.A. (2007) Carbon dioxide dynamics of a restored maritime peatland. *Ecoscience*, 14, 71–80.

Wilson, D., Farell, C., Mueller, C., Hepp, S. & Renou-Wilon, F. (2013) Rewetted industrial cutaway peatlands in western Ireland: a prime location for climate change mitigation? *Mires & Peat*, 11(01), 1–22.

Wilson, D., Blain, D., Couwenberg, J., Evans, C.D., Murdiyarso, D., Page, S.E., Renou-Wilson, F., Rieley, J.O., Sirin, A., Strack, M. & Tuittila, E.-S. (2016a) Greenhouse gas emission factors associated with rewetting of organic soils. *Mires and Peat*, 17(04), 1–28.

Wilson, D., Farrell, C.A., Fallon, D., Moser, G., Müller, C. & Renou-Wilson, F. (2016b) Multiyear greenhouse gas balances at a rewetted temperate peatland. *Global Change Biology*, 22, 4080–4095.

Wohlfahrt, G., Pilloni, S., Hörtnagl, L. & Hammerle, A. (2010) Estimating carbon dioxide fluxes from temperate mountain grasslands using broad-band vegetation indices. *Biogeosciences*, 7, 683–694.

Yu, Z., Beilman, D.W., Frolking, S., MacDonald, G.M., Roulet, N.T., Camill, P. & Charman, D.J. (2011) Peatlands and their role in the global carbon cycle. *Eos, Transactions American Geophysical Union*, 92, 97–98.

Submitted 19 Dec 2017, revision 26 Apr 2018
Editor: David Wilson

Author for correspondence:
Dr Sandhya Karki, Delta Water Management Research Unit, United States Department of Agriculture-ARS, 504 University Loop, Jonesboro, AR 72401, USA.
Tel: +01 870-340-9242; Email: skarki@uark.edu / im.sandhya.karki@gmail.com

 DOI: 10.19189/MaP.2017.DW.322

Appendix

Table A1. Model performance statistics for ecosystem respiration (ER) models fitted to data from flooded (F) treatments.

Model	Data (*n*)	Mean rate simulated	Mean rate observed	Paired *t*-test (*P*)[a]	Correlation (*r*)	Mean bias	Slope	Intercept	*F*-test *(P)*[a]	NSE[b]
ER 1	416	194	191	0.644^{ns}	0.806	-2.3	1.03	-7.1	0.715^{ns}	0.649
ER 2	416	200	191	0.075^{ns}	0.797	-9.0	1.02	-12.4	0.186^{ns}	0.633
ER 3	416	207	191	0.000***	0.921	-15.6	0.93	-0.3	0.000***	0.835
ER 4	416	192	191	0.914^{ns}	0.923	-0.3	1.01	-1.6	0.948^{ns}	0.852
ER 5	416	194	191	0.361^{ns}	0.914	-3.1	1.03	-8.9	0.279^{ns}	0.833
ER 6	416	186	191	0.120^{ns}	0.922	5.0	0.96	12.2	0.048*	0.847
ER 7	416	191	191	0.965^{ns}	0.897	0.2	1.00	0.1	0.999^{ns}	0.805
ER 8	416	193	191	0.750^{ns}	0.907	-1.1	1.00	-0.9	0.949^{ns}	0.822

[a] ns, not significant ($P > 0.05$); *, $P < 0.05$; **, $P < 0.01$; ***, $P < 0.001$; [b] NSE, Nash-Sutcliffe modelling efficiency.

Table A2. Model performance statistics for ecosystem respiration (ER) models fitted to data from semi-flooded (S-F) treatments.

Model	Data (*n*)	Mean rate simulated	Mean rate observed	Paired *t*-test (*P*)[a]	Correlation (*r*)	Mean bias	Slope	Intercept	*F*-test *(P)*[a]	NSE[b]
ER 1	208	258	253	0.508^{ns}	0.880	-4.6	1.04	-7.1	0.715^{ns}	0.649
ER 2	208	272	253	0.011*	0.868	-18.5	1.00	-17.3	0.042*	0.745
ER 3	208	252	253	0.828^{ns}	0.938	1.1	1.06	-14.0	0.089^{ns}	0.877
ER 4	208	256	253	0.581^{ns}	0.940	-2.8	1.02	-7.6	0.654^{ns}	0.884
ER 5	208	257	253	0.488^{ns}	0.940	-3.5	1.03	-10.6	0.446^{ns}	0.882
ER 6	208	251	253	0.659^{ns}	0.940	2.2	0.99	5.6	0.781^{ns}	0.884
ER 7	208	253	253	0.984^{ns}	0.926	-0.1	1.00	-0.1	0.999^{ns}	0.858
ER 8	208	252	253	0.828^{ns}	0.926	1.2	0.96	12.1	0.278^{ns}	0.855

[a] ns, not significant ($P > 0.05$); *, $P < 0.05$; **, $P < 0.01$; ***, $P < 0.001$; [b] NSE, Nash-Sutcliffe modelling efficiency.

Table A3. Model performance statistics for ecosystem respiration (ER) models fitted to data from control (C) treatments.

Model	Data (*n*)	Mean rate simulated	Mean rate observed	Paired *t*-test (*P*)[a]	Correlation (*r*)	Mean bias	Slope	Intercept	*F*-test *(P)*[a]	NSE[b]
ER 1	210	285	280	0.596^{ns}	0.843	-5.1	1.03	-14.1	0.682^{ns}	0.710
ER 2	210	271	280	0.361^{ns}	0.834	9.2	1.18	-39.0	0.003**	0.679
ER 3	210	294	280	0.072^{ns}	0.901	-14.0	0.99	-12.4	0.197^{ns}	0.808
ER 4	210	284	280	0.642^{ns}	0.903	-3.5	1.02	-8.4	0.788^{ns}	0.816
ER 5	210	283	280	0.668^{ns}	0.904	-3.3	1.02	-8.7	0.774^{ns}	0.816
ER 6	210	282	280	0.816^{ns}	0.904	-1.8	1.01	-5.1	0.914^{ns}	0.816
ER 7	210	281	280	0.956^{ns}	0.880	-0.5	1.00	-0.1	0.998^{ns}	0.774
ER 8	210	268	280	0.143^{ns}	0.880	12.4	0.97	21.3	0.225^{ns}	0.771

[a] ns, not significant ($P > 0.05$); *, $P < 0.05$; **, $P < 0.01$; ***, $P < 0.001$; [b] NSE, Nash-Sutcliffe modelling efficiency.

Table A4. Model performance statistics for gross primary production (GPP) models fitted to data from flooded (F) treatments.

Model	Data (*n*)	Mean rate simulated	Mean rate observed	Paired *t*-test (*P*)[a]	Correlation (*r*)	Mean bias	Slope	Intercept	*F*-test *(P)*[a]	NSE[b]
GPP 2	1613	-299	-287	0.000***	0.942	12.5	1.03	20.9	0.000***	0.885
GPP 3	1613	-286	-287	0.844^{ns}	0.945	-0.6	1.00	1.6	0.669^{ns}	0.892
GPP 4	1613	-261	-287	0.000***	0.923	-25.5	0.95	-34.0	0.000***	0.845
GPP 5	1613	-288	-287	0.657^{ns}	0.945	1.4	1.00	2.4	0.829^{ns}	0.894
GPP 6	1613	-304	-287	0.000***	0.946	16.8	0.96	5.5	0.000***	0.891
GPP 7	1613	-283	-287	0.195^{ns}	0.946	-4.1	1.00	-5.4	0.366^{ns}	0.895
GPP 8	1613	-288	-287	0.763^{ns}	0.934	1.0	1.00	0.7	0.950^{ns}	0.873

[a] ns, not significant ($P > 0.05$); *, $P < 0.05$; **, $P < 0.01$; ***, $P < 0.001$; [b] NSE, Nash-Sutcliffe modelling efficiency.

Table A5. Model performance statistics for gross primary production (GPP) models fitted to data from semi-flooded (S-F) treatments.

Model	Data (*n*)	Mean rate simulated	Mean rate observed	Paired *t*-test (*P*)[a]	Correlation (*r*)	Mean bias	Slope	Intercept	*F*-test *(P)*[a]	NSE[b]
GPP 2	805	-333	-323	0.025*	0.947	10.7	1.03	20.6	0.005**	0.895
GPP 3	805	-319	-323	0.407^{ns}	0.949	-3.9	1.01	-0.7	0.503^{ns}	0.900
GPP 4	805	-297	-323	0.000***	0.931	-25.5	0.95	-39.0	0.000***	0.862
GPP 5	805	-325	-323	0.531^{ns}	0.951	2.9	1.00	2.9	0.822^{ns}	0.905
GPP 6	805	-336	-323	0.003**	0.951	13.5	0.97	4.1	0.001***	0.903
GPP 7	805	-319	-323	0.442^{ns}	0.951	-3.5	0.99	-6.7	0.504^{ns}	0.904
GPP 8	805	-332	-323	0.047*	0.942	9.8	0.99	6.4	0.101^{ns}	0.887

[a] ns, not significant ($P > 0.05$); *, $P < 0.05$; **, $P < 0.01$; ***, $P < 0.001$; [b] NSE, Nash-Sutcliffe modelling efficiency.

Table A6. Model performance statistics for gross primary production (GPP) models fitted to data from control (C) treatments.

Model	Data (*n*)	Mean rate simulated	Mean rate observed	Paired *t*-test (*P*)[a]	Correlation (*r*)	Mean bias	Slope	Intercept	*F*-test *(P)*[a]	NSE[b]
GPP 2	793	-353	-337	0.001**	0.955	15.9	1.01	19.4	0.003**	0.911
GPP 3	793	-334	-337	0.514^{ns}	0.957	-3.1	1.01	1.7	0.339^{ns}	0.915
GPP 4	793	-300	-337	0.000***	0.930	-36.3	0.95	-52.5	0.000***	0.856
GPP 5	793	-336	-337	0.902^{ns}	0.960	-0.6	1.00	0.9	0.907^{ns}	0.921
GPP 6	793	-348	-337	0.013**	0.960	11.4	0.97	0.6	0.000***	0.921
GPP 7	793	-334	-337	0.586^{ns}	0.960	-2.5	0.99	-5.2	0.622^{ns}	0.922
GPP 8	793	-338	-337	0.880^{ns}	0.948	0.8	1.00	2.4	0.912^{ns}	0.898

[a] ns, not significant ($P > 0.05$); *, $P < 0.05$; **, $P < 0.01$; ***, $P < 0.001$; [b] NSE, Nash-Sutcliffe modelling efficiency.